JACS
JOURNAL OF THE AMERICAN CHEMICAL SOCIETY
Article
pubs.acs.org/JACS

Controlling Switching in Bistable [2]Catenanes by Combining Donor–Acceptor and Radical–Radical Interactions

Zhixue Zhu,[†] Albert C. Fahrenbach,[†,‡] Hao Li,[†] Jonathan C. Barnes,[†,‡] Zhichang Liu,[†] Scott M. Dyar,[†,§] Huacheng Zhang,[†] Juying Lei,[†] Raanan Carmieli,[†,§] Amy A. Sarjeant,[†] Charlotte L. Stern,[†] Michael R. Wasielewski,[†,§] and J. Fraser Stoddart*[,†,‡]

[†]Department of Chemistry, Northwestern University, 2145 Sheridan Road, Evanston, Illinois 60208, United States

[‡]NanoCentury KAIST Institute and Graduate School of EEWS (WCU), Korea Advanced Institute of Science and Technology, 373-1 Guseong Dong, Yuseong Gu, Daejeon 305-701, Republic of Korea

[§]Argonne-Northwestern Solar Energy Research (ANSER) Center, Northwestern University, Evanston, Illinois 60208, United States

Supporting Information

ABSTRACT: Two redox-active bistable [2]catenanes composed of macrocyclic polyethers of different sizes incorporating both electron-rich 1,5-dioxynaphthalene (DNP) and electron-deficient 4,4′-bipyridinium ($BIPY^{2+}$) units, interlocked mechanically with the tetracationic cyclophane cyclobis(paraquat-*p*-phenylene) ($CBPQT^{4+}$), were obtained by donor–acceptor template-directed syntheses in a threading-followed-by-cyclization protocol employing Cu(I)-catalyzed azide–alkyne 1,3-dipolar cycloadditions in the final mechanical-bond forming steps. These bistable [2]catenanes exemplify a design strategy for achieving redox-active switching between two translational isomers, which are driven (i) by donor–acceptor interactions between the $CBPQT^{4+}$ ring and DNP, or (ii) radical–radical interactions between $CBPQT^{2(\bullet+)}$ and $BIPY^{\bullet+}$, respectively. The switching processes, as well as the nature of the donor–acceptor interactions in the ground states and the radical–radical interactions in the reduced states, were investigated by single-crystal X-ray crystallography, dynamic ^{1}H NMR spectroscopy, cyclic voltammetry, UV/vis spectroelectrochemistry, and electron paramagnetic resonance (EPR) spectroscopy. The crystal structure of one of the [2]catenanes in its trisradical tricationic redox state provides direct evidence for the radical–radical interactions which drive the switching processes for these types of mechanically interlocked molecules (MIMs). Variable-temperature ^{1}H NMR spectroscopy reveals a degenerate rotational motion of the $BIPY^{2+}$ units in the $CBPQT^{4+}$ ring for both of the two [2]catenanes, that is governed by a free energy barrier of 14.4 kcal mol^{-1} for the larger catenane and 17.0 kcal mol^{-1} for the smaller one. Cyclic voltammetry provides evidence for the reversibility of the switching processes which occurs following a three-electron reduction of the three $BIPY^{2+}$ units to their radical cationic forms. UV/vis spectroscopy confirms that the processes driving the switching are (i) of the donor–acceptor type, by the observation of a 530 nm charge-transfer band in the ground state, and (ii) of the radical–radical ilk in the switched state as indicated by an intense visible absorption (ca. 530 nm) and near-infrared (ca. 1100 nm) bands. EPR spectroscopic data reveal that, in the switched state, the interacting $BIPY^{\bullet+}$ radical cations are in a fast exchange regime. In general, the findings lay the foundations for future investigations where this radical–radical recognition motif is harnessed in bistable redox-active MIMs in order to achieve close to homogeneous populations of co-conformations in both the ground and switched states.

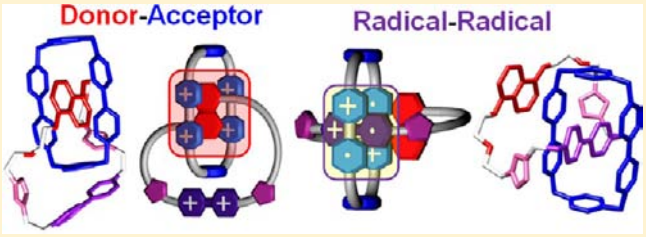

INTRODUCTION

With our growing understanding of molecular recognition processes[1] and their use in aiding and abetting self-assembly processes,[2] mechanically interlocked molecules[3] (MIMs), such as catenanes,[4] rotaxanes,[5] and some unique topological molecules such as Borromean rings[6] and Solomon links,[7] have been synthesized in high yields by employing template-directed protocols[8] which rely on noncovalent bonding interactions.[9] These protocols relate to supramolecular assistance to covalent syntheses.[10] Among the MIMs, redox-active bistable catenanes and rotaxanes, derived from the π-electron-deficient cyclobis(paraquat-*p*-phenylene) ($CBPQT^{4+}$) ring,[11] interlocked with a ring or dumbbell component incorporating π-electron-rich donor units, have attracted considerable attention on account of their possible applications and potential for use in molecular electronic devices,[12] nanoelectromechanical systems,[13] and mechanized nanoparticles.[14]

We have helped to produce[15] a blueprint over the years for the construction of bistable MIMs of the donor–acceptor redox-active ilk, which, by necessity have two non-degenerate recognition sites for the $CBPQT^{4+}$ ring, one of which must display reversible redox chemistry. In the ground state, these

Received: April 18, 2012
Published: July 6, 2012

dx.doi.org/10.1021/ja3037355 | J. Am. Chem. Soc. 2012, 134, 11709–11720

bistable MIMs exhibit a distribution of co-conformations governed by the relative affinities of the two donor recognition units for the $CBPQT^{4+}$ ring component. The distribution of the ring can be switched by oxidizing reversibly the recognition unit with the greater affinity for the ring. For example, we have reported[15c] a bistable donor–acceptor [2]catenane composed of two different π-donors—namely, tetrathiafulvalene (TTF) and 1,5-dioxynaphthalene (DNP) units in a macrocyclic polyether, mechanically interlocked with the $CBPQT^{4+}$ ring—which demonstrates excellent translational selectivity,[16] that is, approximately 150:1. More recently, Liu et al.[17] have investigated bistable [2]catenanes composed of the π-electron-rich 1,5-dinaphtho[38]crown-10 as the degenerate ring component, together with a rigid cyclophane incorporating the electron-deficient 4,4′-bipyridinium dication ($BIPY^{2+}$) and a neutral unit which was either naphthalene diimide (NDI) or pyromellitic diimide (PMI). These MIMs exhibit co-conformational selectivity (over 97:3) on account of the stronger donor–acceptor interactions of the crown ether ring with the $BIPY^{2+}$ unit. In both of these examples, the ground state displays a distribution of translational isomers as a consequence of the design of the MIMs. A design strategy which avoids such a ground-state distribution for these types of bistable MIMs remains to be uncovered.

Recently, we discovered[18] that positively charged $BIPY^{2+}$ units and the $CBPQT^{4+}$ ring form strong inclusion complexes after all their $BIPY^{2+}$ units have been reduced to their radical cationic forms. These inclusion complexes are stabilized by radical–radical interactions[18b] between their three $BIPY^{\bullet+}$ radical cation components. Furthermore, when it has the diradical dicationic form, the $CBPQT^{2(\bullet+)}$ ring loses[19] its non-covalent donor–acceptor affinity for π-electron-rich units such as DNP. Likewise, in their fully oxidized forms, $BIPY^{2+}$ units and $CBPQT^{4+}$ rings lose all their affinity for each other as a consequence of Coulombic repulsion: indeed $BIPY^{2+}$ units serve[20] as electrostatic barriers in contrast to providing stable co-conformations. The incorporation of $BIPY^{2+}$ and DNP as two recognition units in a molecular switch constitutes (Figure 1) *a step forward in devising a strategy for designing a bistable MIM which avoids any population of minor co-conformations in either its ground or switched states.*

Herein, we discuss the strategy we have employed in the synthesis of two new [2]catenanes for defining bistable MIMs with near quantitative translational selectivity in both the ground and switched states. The two new catenanes—composed of macrocyclic polyethers containing both electron-rich DNP and electron-deficient $BIPY^{2+}$ recognition units mechanically interlocked with the $CBPQT^{4+}$ ring—demonstrate reversible switching behavior, relying upon the donor–acceptor interactions of the $CBPQT^{4+}$ ring with DNP entities in the ground state, and selective radical–radical interactions of $CBPQT^{2(\bullet+)}$ with $BIPY^{\bullet+}$ entities in the reduced state. The switching behavior of these [2]catenanes has been characterized by X-ray crystallography and UV/vis, ^{1}H NMR, and EPR spectroscopies in addition to cyclic voltammetry. Furthermore, we have identified and investigated the rate of degenerate motion of the $BIPY^{2+}$ units of the $CBPQT^{4+}$ ring, which is affected by the size of the macrocyclic polyether influencing the amount of Coulombic repulsion from the positively charged $BIPY^{2+}$ unit that functions as an electrostatic barrier.

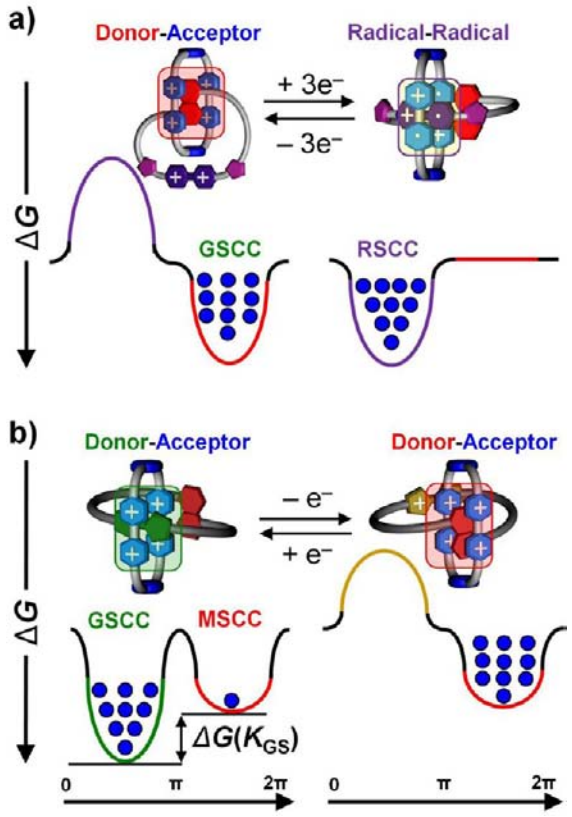

Figure 1. (a) Design strategy for achieving redox-active bistability in a [2]catenane which takes advantage of donor–acceptor and radical–radical interactions. In the ground state, donor–acceptor interactions between the π-electron-rich DNP unit of the macrocyclic polyether and the $BIPY^{2+}$ units of the $CBPQT^{4+}$ ring dominate, as illustrated by the free energy profile. The $BIPY^{2+}$ unit of the macrocyclic polyether resists inclusion inside the cavity of $CBPQT^{4+}$ as a consequence of Coulombic repulsion. After reduction of the $CBPQT^{4+}$ ring and the $BIPY^{2+}$ unit of the macrocyclic polyether to their radical cationic forms, $BIPY^{\bullet+}$ radical–radical interactions drive the switching of the $CBPQT^{2(\bullet+)}$ ring. In its diradical dicationic form, the $CBPQT^{2(\bullet+)}$ ring has no affinity for the DNP unit. (b) Traditional design strategy for achieving redox-active bistable [2]catenanes, which relies on donor–acceptor interactions in both redox states. By necessity, the ground state exists as a distribution of translational isomers that is governed by the relative affinities of the two donor units for the cavity of the $CBPQT^{4+}$ ring.

RESULTS AND DISCUSSIONS

Synthesis and Design Strategy. The macrocyclic polyethers **3**·$2PF_6$ and **5**·$2PF_6$ incorporating DNP and $BIPY^{2+}$ units were synthesized in order to allow us to investigate the strength of their intramolecular donor–acceptor interactions. Their syntheses, which rely upon copper(I)-catalyzed azide–alkyne cycloadditions[21] (CuAAC) of the dialkyne **1**·$2PF_6$ with either the diazide **2** or **4** under high dilution conditions, afforded (Scheme 1) **3**·$2PF_6$ and **5**·$2PF_6$, respectively, as red solids in 32 and 35% yield. The red color of the compounds is the result of an intramolecular donor–acceptor charge transfer from the highest occupied molecular orbital (HOMO) of the DNP unit to the lowest unoccupied molecular orbital (LUMO) of the $BIPY^{2+}$ unit, which is confirmed[22] by the weak absorption band centered at 530 nm in MeCN solution. This strong intramolecular interaction is also reflected in significant shifts in the δ values of the resonances for the aromatic protons

dx.doi.org/10.1021/ja3037355 | J. Am. Chem. Soc. 2012, 134, 11709–11720

Scheme 1. Syntheses of the Two Free Macrocyclic Polyethers 3·2PF$_6$ and 5·2PF$_6$ and Template-Directed Syntheses of the Two [2]Catenanes 6·6PF$_6$ and 7·6PF$_6$, Respectively, Employing a Threading-Followed-by-Cyclization Protocol[a]

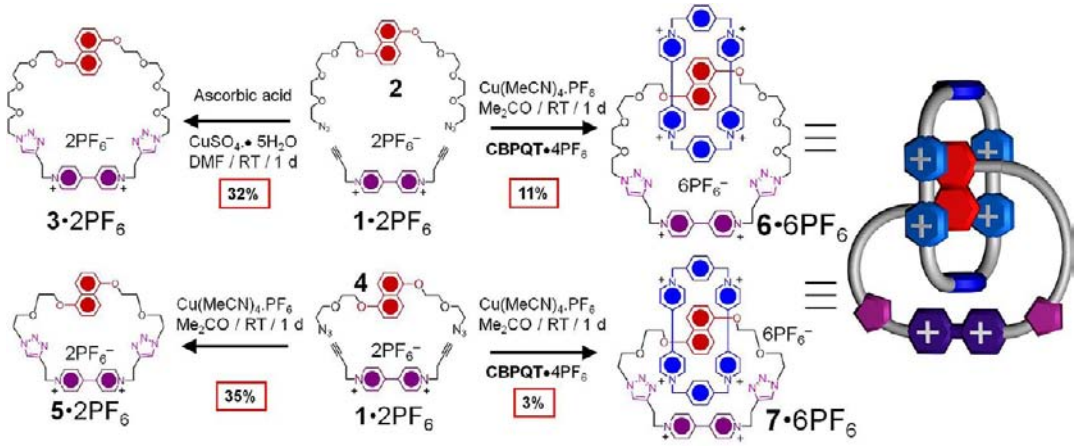

[a]Each reaction employs the Cu(I)-catalyzed 1,3-dipolar cycloaddition between the terminal alkynes of **1**·2PF$_6$ and the azides of **2** or **4**.

in the ^{1}H NMR spectra (see SI) compared with those for their individual components **1**·2PF$_6$ and **2** and their 1:1 complex at a 9 mM concentration.

Single-crystal X-ray analyses revealed that the DNP and BIPY^{2+} units in both **3**$^{2+}$ and **5**$^{2+}$ enter into face-to-face stacking with each other as a consequence of favorable donor–acceptor interactions, resulting in the closing up of the cavities for these macrocyclic polyethers (see SI). It follows that, when implementing the clipping approach to the formation of the mechanical bond, a high energy barrier has to be overcome in order to open up the closed cavity of the macrocyclic polyether such that catenation can ensue. Attempts at catenations by using a conventional clipping[8,23] strategy, involving the reaction of 1,4-bis(bromomethyl)benzene and 1,1′-[1,4-phenylenebis-(methylene)]bis(4,4′-bipyridinium)bis(hexafluorophosphate) in the presence of **3**·2PF$_6$ and **5**·2PF$_6$ as templates, were carried out. In anticipation of the tricationic intermediate being formed prior to closure of the CBPQT^{4+} ring, we hypothesized that catenation[24] can occur even in the presence of the dicationic BIPY^{2+} units of the self-complexing macrocyclic polyethers **3**·2PF$_6$ and **5**·2PF$_6$. None of the desired catenanes were formed during this reaction, however, indicating that the intramolecular donor–acceptor interactions are presumably much greater than the intermolecular donor–acceptor interactions between the tricationic intermediate and the DNP unit.

In order to minimize the influence of the *intra*molecular recognition processes in the macrocyclic polyethers, which compete with *inter*molecular ones during the template-directed syntheses, we examined catenation using a threading-followed-by-cyclization approach. ^{1}H NMR titration of equimolar amounts of **2** and CBPQT·4PF$_6$ at 9 mM showed (see SI) large upfield shifts of the DNP protons H$_{2/6}$ and H$_{3/7}$ by approximately 0.8 and 1.5 ppm, respectively, and H$_{4/8}$ by 5.4 ppm. The complexation of **2** and CBPQT·4PF$_6$ was not affected by adding 1.0 equiv of **1**·2PF$_6$ to the solution, indicating that **1**·2PF$_6$ is not involved in the competitive binding process. Encouraged by this result, the [2]catenane **6**·6PF$_6$ was obtained (Scheme 1) in 11% yield by a macrocyclization of the complex **2**⊂CBPQT·4PF$_6$ and **1**·2PF$_6$ in a 1:1:1 ratio catalyzed by Cu(I) at room temperature under high dilution conditions (10 mM for each component). The low yield is ascribed to the energetically costly influence of Coulombic repulsion between the BIPY^{2+} unit of the acyclic polyether intermediate and CBPQT^{4+} during the cyclization process. The [2]catenane **7**·6PF$_6$ was prepared in a similar fashion in 3% yield by a cyclization of complex **4**⊂CBPQT·4PF$_6$ and **1**·2PF$_6$ in a 1:1:1 ratio of each of the components. The much smaller ring size in the case of **7**·6PF$_6$, compared with that of **6**·6PF$_6$, forces the positively charged BIPY^{2+} units into even closer proximity with the CBPQT^{4+} ring, a situation which likely raises the conformational transition-state energies of the cyclization leading to a lower yield of this [2]catenane. The [2]catenanes **6**·6PF$_6$ and **7**·6PF$_6$ were characterized by ^{1}H, ^{13}C, and ^{1}H–^{1}H COSY NMR spectroscopies (Figure 2 and SI) as well as by high-resolution mass spectrometry.

X-ray Crystallography. The fact that the CBPQT^{4+} rings and BIPY^{2+} units are mutually repulsive in their fully oxidized forms has been investigated thoroughly in rotaxanes as well as in their pseudorotaxane precursors. If the CBPQT^{4+} ring must

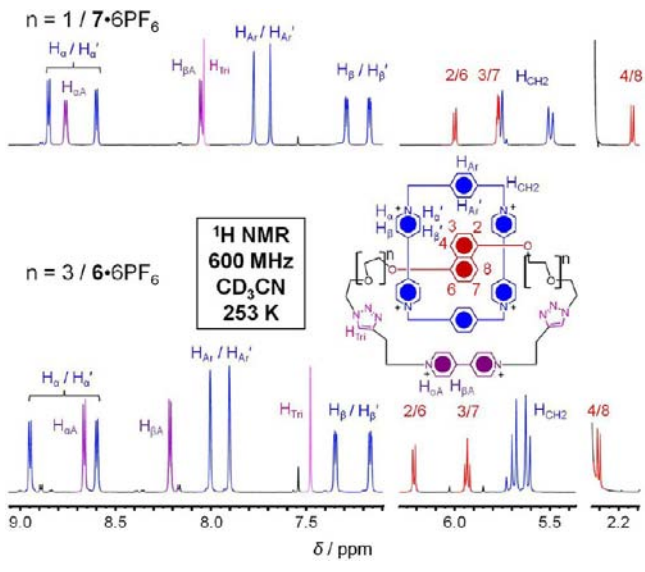

Figure 2. Partial ^{1}H NMR spectra of (top) **7**·6PF$_6$ and (bottom) **6**·6PF$_6$. Assignments of the resonances were made with the assistance of data from 2D ^{1}H–^{1}H COSY experiments.

dx.doi.org/10.1021/ja3037355 | J. Am. Chem. Soc. 2012, 134, 11709–11720

pass over $BIPY^{2+}$ units in order to encircle a π-electron-rich unit, in the case of either rotaxanes[20b−e] or pseudorotaxanes,[20e] the rate of shuttling or that of complex formation is decreased by many orders of magnitude as a consequence of electrostatic repulsion, which greatly increases the transition state energies for these processes. Little is known, however, about the nature of these repulsive interactions in the solid-state. Single crystals suitable for X-ray diffraction[25,26] were grown (i) by vapor diffusion of iPr_2O into a solution of $\mathbf{6}\cdot 6PF_6$ in MeCN and by (ii) vapor diffusion of Et_2O into a solution of $\mathbf{7}\cdot 6PF_6$ in Me_2CO. The solid-state structures of $\mathbf{6}^{6+}$ and $\mathbf{7}^{6+}$ are illustrated in Figure 3.

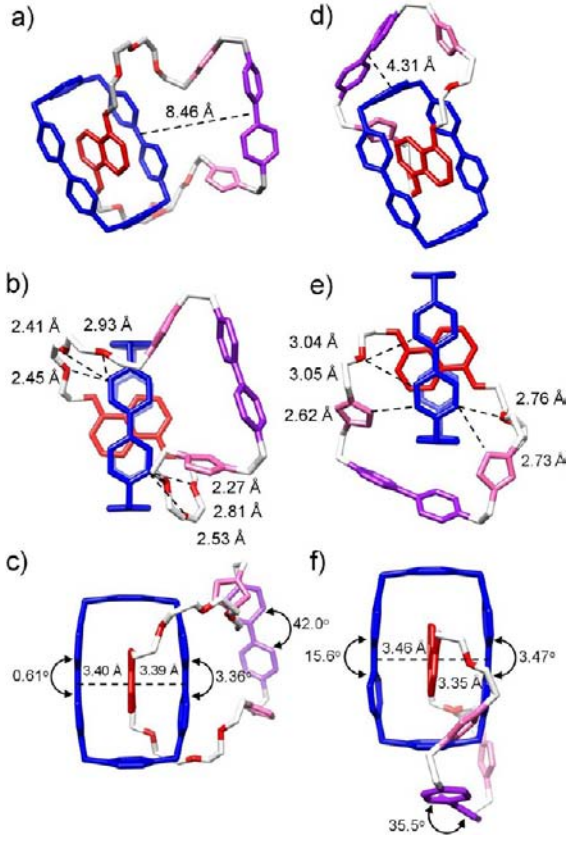

Figure 3. Different views of the solid-state structures of the [2]catenanes $\mathbf{6}^{6+}$ (a−c) and $\mathbf{7}^{6+}$ (d−f) in their ground states. The PF_6^- counterions and solvent molecules have been omitted for the sake of clarity. In (b) and (e), the distances labeled are those measured from the proton and oxygen/nitrogen atoms of the [C−H···O] and [C−H···N] interactions, despite the fact that the hydrogen atoms have been removed for clarity's sake.

In the case of $\mathbf{6}^{6+}$, the unit cell of the crystal is monoclinic and belongs to the $C2/c$ space group. The DNP unit of the macrocyclic polyether component resides inside the cavity of the $CBPQT^{4+}$ ring in an almost centrosymmetric fashion, separated by distances which are characteristic of π-associated donor−acceptor interactions—namely, 3.40 and 3.39 Å from the two $BIPY^{2+}$ units in the ring. The protons on $C_{4/8}$ of the DNP unit are engaged in [C−H···π] interactions[20d,27] with the phenylene units of the $CBPQT^{4+}$ ring, a structural feature which places these 4/8 protons directly in the shielding zone of the phenylene rings, resulting in their substantial upfield ^1H NMR chemical shifts. Overall, this type of structural arrangement is one which is commonly observed[27] for DNP units located inside the cavity of the $CBPQT^{4+}$ ring. The $BIPY^{2+}$ unit in the macrocyclic polyether is located distant from the tetracationic cyclophane. A distance of 8.46 Å spans the gap between the centroids of the $BIPY^{2+}$ unit of the macrocyclic polyether and the closer of the two $BIPY^{2+}$ units of the $CBPQT^{4+}$ ring. This large distance is a consequence of Coulombic repulsion and is consistent[20] with our previous investigations, which have demonstrated that $BIPY^{2+}$ units serve as electrostatic barriers for the $CBPQT^{4+}$ ring. In addition to donor−acceptor π-stacking and [C−H···π] interactions, the second, third and fourth oxygen atoms of the polyether ring are engaged in [C−H···O] interactions with the relatively acidic protons on the carbon atoms α to the formally positive nitrogen atoms of the $CBPQT^{4+}$ ring. The distances between the acidic α protons and the oxygen atoms range from approximately 2.2 to 3.0 Å. These [C−H···O] interactions are similar[27,28] to those commonly observed in previously investigated systems involving the $CBPQT^{4+}$ ring and DNP units functionalized with oligoethylene glycol chains. Other important structural features of note are the torsional angles of the $BIPY^{2+}$ units. In their dicationic forms, $BIPY^{2+}$ units commonly adopt relatively large torsional angles (~35°) between the mean planes of their two pyridinium rings. The torsional angle of the $BIPY^{2+}$ unit in the macrocyclic polyether is 42°. When the LUMO of the $BIPY^{2+}$ unit becomes populated[29] with electrons donated from the HOMO of π-electron-rich species, however, the central aryl C−C bond takes on double-bond character and is decreased in length. This trend happens as a consequence of the antibonding nature of the LUMO, which acts to shorten the length of some C−C bonds, while elongating others in a manner that leads to an overall reduction of the bond order in the $BIPY^{2+}$ unit. The consequence of the central aryl C−C bond assuming double-bond character is that free rotation about this bond is hindered, and the two pyridinium units become increasingly coplanar with one another. Hence, the torsional angles of the $BIPY^{2+}$ units serve as indicators for donor−acceptor interactions. The torsional angles of the two $BIPY^{2+}$ units of the $CBPQT^{4+}$ ring are both much less—between 0 and 4°—than that in the macrocyclic polyether as a result of donor−acceptor interactions with the included DNP unit.

In the case of $\mathbf{7}^{6+}$, the unit cell of the crystal is monoclinic and belongs to the $P2_1/n$ space group. The DNP unit resides in an almost centrosymmetric fashion inside the cavity of the $CBPQT^{4+}$ ring, although it deviates more than its larger analogue, since it is located closer to one side (3.35 Å) of the ring than to the other (3.46 Å). The $BIPY^{2+}$ unit in the $CBPQT^{4+}$ ring closer to the DNP unit reveals a smaller torsional angle (3.5°) compared to that (16°) of the $BIPY^{2+}$ farther away. The protons on $C_{4/8}$ of the DNP unit are also found to be engaged in [C−H···π] interactions with the phenylene linkers in the $CBPQT^{4+}$ ring. The $BIPY^{2+}$ unit in the macrocyclic polyether is situated much closer to the $CBPQT^{4+}$ ring, alongside one of its two phenylene units with a distance of 4.31 Å separating their respective centroids. Since the small circumference of the macrocyclic polyether places considerable geometric constraints on the location of the $BIPY^{2+}$ unit, the fact that it lies close in proximity to one of the phenylene linkers in the $CBPQT^{4+}$ ring is most likely because of its tendency to minimize Coulombic repulsions. The relatively large torsional angle (36°) of the $BIPY^{2+}$ unit in the macrocyclic polyether indicates little to no π-donor−acceptor type interactions with the phenylene unit in the $CBPQT^{4+}$ ring,

dx.doi.org/10.1021/ja3037355 | J. Am. Chem. Soc. 2012, 134, 11709−11720

and its close proximity is solely a result of the geometric constraints of the crown ether, while minimizing Coulombic repulsions. This kind of co-conformation stands out in stark contrast to the co-conformations observed in catenanes where two *donor* units are incorporated into the macrocyclic polyether. In these cases,[15c,27a,30] where the secondary donor unit does not reside inside the cavity of the $CBPQT^{4+}$ ring, it is nonetheless situated comfortably alongside one of the $BIPY^{2+}$ units in order to maximize favorable $\pi-\pi$ stacking interactions. This intercomponent interaction effectively leads to an *inside* and *outside* $BIPY^{2+}$ unit. In the case of $7{\cdot}6PF_6$, Coulombic repulsion mitigates against this type of co-conformation, and instead we observe a co-conformation which has inside and outside *phenylene* units. The triazole units of 7^{6+} also appear to play a significant role as hydrogen bond acceptors, a situation which is not the case for $\mathbf{6}^{6+}$. The closer proximity of the triazole units for 7^{6+}, brought about by the smaller geometric circumference of the macrocyclic polyether, promotes their ability to form [C−H···N] interactions with the acidic α protons of one of the $BIPY^{2+}$ units in the $CBPQT^{4+}$ ring. Distances of ∼2.6−2.7 Å characterize the separation between the nitrogen atoms in the 2-position of the two triazole rings with the α protons of the $CBPQT^{4+}$ ring. The more typical [C−H···O] interactions between the second oxygen atoms of the polyether loop with the α, as well as the β, protons on a $BIPY^{2+}$ unit are also observed. The three-dimensional superstructures associated with the crystal packing in $\mathbf{6}^{6+}$ and 7^{6+} are both highly ordered (see the cif files).

The solid-state structure of the [2]catenane 7^{6+} in its reduced trisradical tricationic redox state $7^{3(\bullet+)}$ was also investigated. We employed zinc dust as a heterogeneous reducing agent since it is known to reduce[31] $BIPY^{2+}$ units to their $BIPY^{\bullet+}$ radical cationic forms. Single crystals suitable for X-ray diffraction analysis were obtained[32] by slow vapor diffusion of $i\mathrm{Pr}_2\mathrm{O}$ into a purple MeCN solution of $7^{3(\bullet+)}$ as its PF_6^- salt. The solid-state structure of the purple plate crystals which grew revealed (Figure 4), first of all, that the [2]catenane had indeed been reduced to its trisradical form by the observation of three PF_6^- counterions in the solid-state superstructure per [2]catenane. The $BIPY^{\bullet+}$ radical cation in the macrocyclic polyether resides inside the cavity of the $CBPQT^{2(\bullet+)}$ ring as a consequence of favorable radical−radical interactions with its $BIPY^{\bullet+}$ radical cations. In contrast to a previously studied inclusion complex[18b] involving the methyl viologen radical cation included inside the cavity of the $CBPQT^{2(\bullet+)}$ ring, the $BIPY^{\bullet+}$ unit in the crown ether deviates significantly from a centrosymmetric occupancy. Specifically, the $BIPY^{\bullet+}$ is located significantly closer to one side (3.08 Å) of the $CBPQT^{2(\bullet+)}$ ring than the other (3.40 Å), and one pyridinium ring is located more closely toward the center of the cavity than the other. This deviation from centrosymmetry is most likely a consequence of the constrained geometry of the macrocyclic polyether, as well as the [C−H···O] and [C−H···N] interactions, which only occur on one side of the macrocyclic polyether whereas they are absent on the other. In addition, the $BIPY^{\bullet+}$ unit is bowed, with the terminal methylene-to-nitrogen bonds subtending an angle of ∼170°—a deviation of 10° from the conventional linear geometry of a $BIPY^{\bullet+}$ unit. Since a radical electron populates each of their antibonding orbitals, the torsional angles of the $BIPY^{\bullet+}$ radical cation units tend toward zero—as is the case for donor−acceptor interactions (*vide supra*). The fact that the torsional angles of all the $BIPY^{\bullet+}$ units are less than 7° is another indication that these units are indeed in their radical

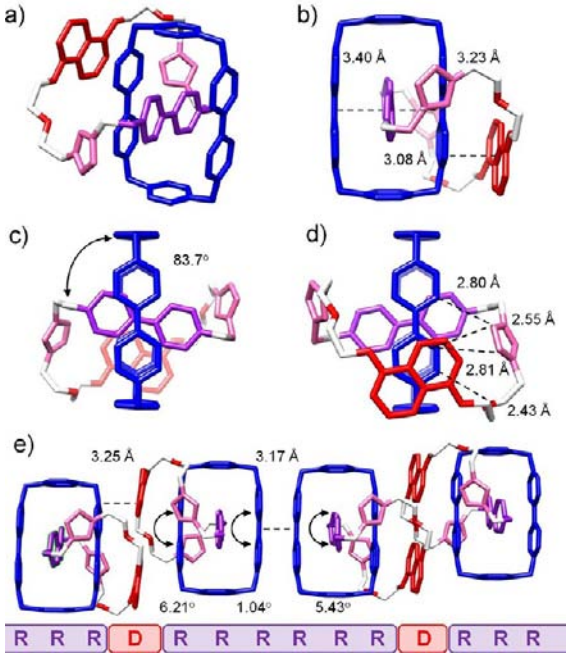

Figure 4. Different views (a−d) of the solid-state structure of the trisradical tricationic $7^{3(\bullet+)}$ and (e) a view of its superstructure displaying the packing arrangement between adjacent $7^{3(\bullet+)}$ molecules. The PF_6^- counterions and solvent molecules have been omitted for the sake of clarity. In the illustration, R stands for a radical cationic unit and D stands for a π-electron donor unit. In (d), the distances labeled are those measured from the hydrogen to the oxygen/nitrogen atoms of the [C−H···O]/[C−H···N] interactions despite the fact that the hydrogen atoms have been removed for clarity's sake.

cationic forms. The DNP unit of the macrocyclic polyether is located alongside one of the $BIPY^{\bullet+}$ units in the $CBPQT^{2(\bullet+)}$ ring, separated by a plane-to-plane distance of 3.25 Å. In contrast to the way alongside DNP units typically interact[27] with $BIPY^{2+}$ units in their dicationic form, the DNP unit of $7^{3(\bullet+)}$ and the $BIPY^{\bullet+}$ radical cation are offset by an amount more than what is typically observed. Instead, the DNP unit is located far off to one side of the $BIPY^{\bullet+}$ of the $CBPQT^{2(\bullet+)}$ ring, partially overlapping with only one of the pyridinium rings, extending toward the methylene carbons. This observation can be explained by the fact that DNP units interact only very weakly at best with $BIPY^{\bullet+}$ units when they are in their radical cationic states. The fact that there is any interaction at all is most likely a result of the constraining geometry of the relatively small crown ether. The superstructure of $7^{3(\bullet+)}$ reveals an unusual packing geometry. Two neighboring $7^{3(\bullet+)}$ catenanes in the trisradical state are held together by the alongside $BIPY^{\bullet+}$ units of the $CBPQT^{2(\bullet+)}$ ring components, with a centroid-to-centroid separation of 3.17 Å between these adjacent $BIPY^{\bullet+}$ units. The DNP units stack with the inside $BIPY^{\bullet+}$ radical cations from an adjacent catenane, overlapping with the remaining pyridinium ring not already interacting intramolecularly with its own DNP unit. Overall, the superstructure of $7^{3(\bullet+)}{\cdot}3PF_6$ is arranged (Figure 4e) in an infinite stack of D-R-R-R-R-R-R-D, where D and R denote donor DNP and $BIPY^{(\bullet+)}$ radical cation, respectively. The three-dimensional superstructure of $7^{3(\bullet+)}$ is also highly ordered in the crystal packing. This crystal structure provides structural evidence for the basis of radical−radical interactions utilized in the template-directed synthesis of rotaxanes[33] and their

dx.doi.org/10.1021/ja3037355 | J. Am. Chem. Soc. 2012, 134, 11709−11720

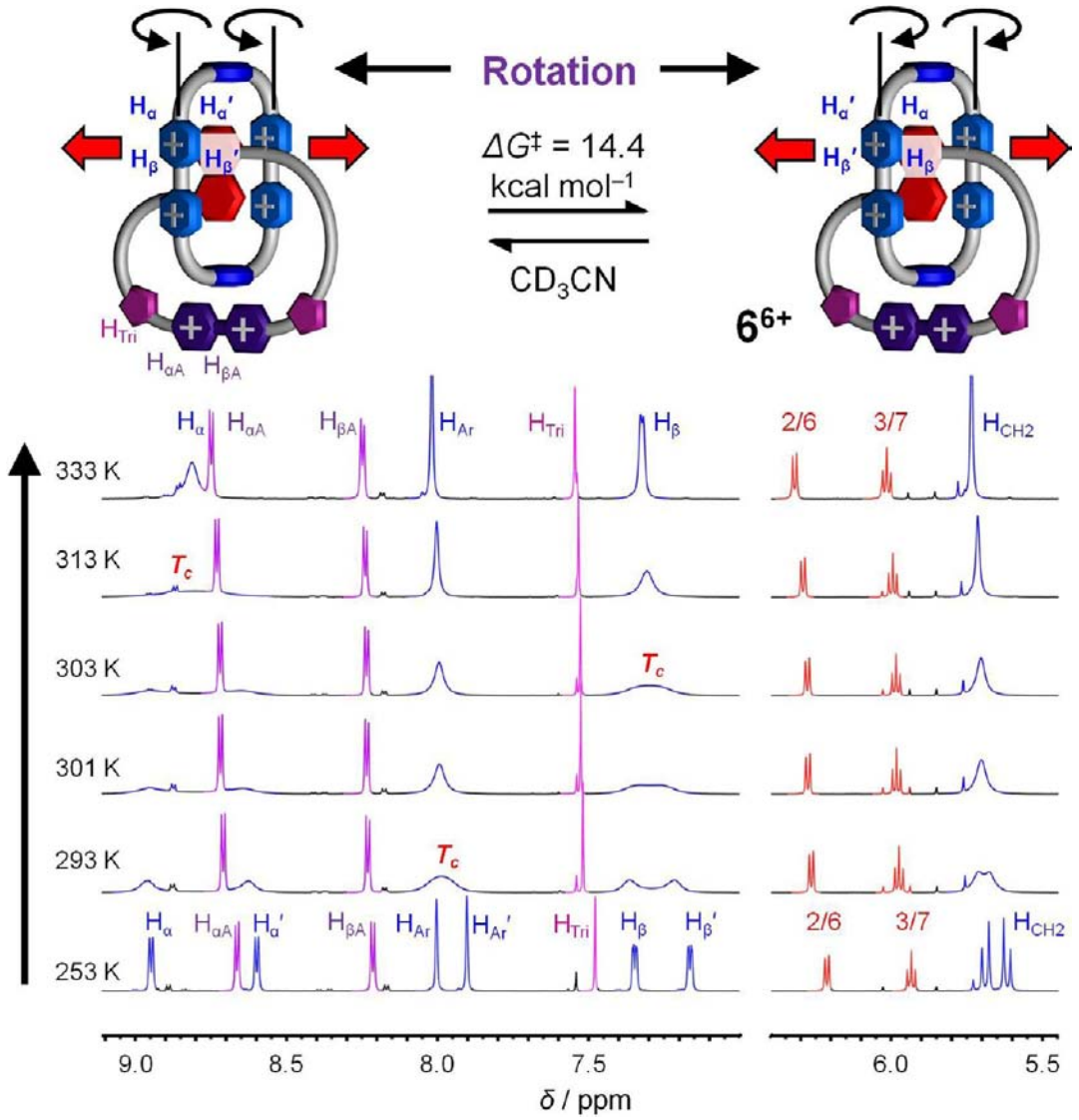

Figure 5. Partial variable-temperature ^{1}H NMR spectra of **6**·6PF$_6$ recorded in CD_3CN. Coalescence temperatures for different pairs of exchanging resonances are indicated on the spectra as T_c.

switching.[34] We further speculate that the imposition of the DNP unit along the π-stacking axis may lead to atypical charge-transport properties in the context of field effect transistors, which we are currently investigating.

^{1}H NMR Spectroscopy. We have employed dynamic ^{1}H NMR spectroscopy to probe (Figure 5) the conformational and co-conformational behavior of **6**$^{6+}$ and **7**$^{6+}$ in their fully oxidized states. First of all, the resonances of $H_{4/8}$ on the DNP units are shifted upfield dramatically to $\delta \approx 2.2$ ppm in the case of both catenanes. These large upfield shifts are a result of [C−H···π] interactions of these protons with the phenylene linkers in the CBPQT^{4+} ring—an observation which confirms the DNP unit is encircled by the CBPQT^{4+} ring in solution. All the other resonances observed in the aromatic region of the ^{1}H NMR spectra have been assigned (see SI) using ^{1}H−^{1}H correlation spectroscopy. It is important to note the presence of two separate resonances for both the α and β protons of the CBPQT^{4+} rings at low temperatures. This doubling up of these signals is a consequence of the DNP unit imposing its local C_{2h} symmetry on the CBPQT^{4+} ring, resulting in a two-fold separation of the signals associated with α and β protons on each BIPY^{2+} unit of the rings. At low temperatures, the degenerate rotational motions of the BIPY^{2+} and DNP units which exchanges these protons between different chemical environments above room temperature, becomes slow on the ^{1}H NMR time scale. In addition, we must consider the influence of co-conformational changes on the resulting proton chemical environment. It may be recalled that, in the solid-state of **7**$^{6+}$, the dicationic BIPY^{2+} unit of the macrocyclic polyether enters into a close stacking-like geometry with one of the phenylene units of the CBPQT^{4+} ring, such that there are no longer inside and outside BIPY^{2+} units associated with the CBPQT^{4+} ring, but rather inside and outside phenylene units. One piece of evidence which supports the existence of this co-conformation in solution is that the chemical shifts of the resonances assigned to the phenylene protons are shifted upfield in comparison with those in the larger catenane, evidence[35] which suggests an enhanced shielding effect caused by the enforced proximity of the BIPY^{2+} unit to one of the phenylene units in **7**$^{6+}$ compared to the situation in **6**$^{6+}$. This co-conformation would lead to a further doubling of the signals for the α and β protons. Hence, in the slow-exchange limit, we

dx.doi.org/10.1021/ja3037355 | J. Am. Chem. Soc. 2012, 134, 11709−11720

would expect to see a total of four α and four β proton resonances, respectively, for the CBPQT^{4+} ring. Even at low temperatures, however, we are only able to observe a pair of resonances for both the α and β protons, indicating that the degenerate pirouetting motion of the polyether loop is always fast on the ^{1}H NMR time scale under the experimental conditions we have employed so far. Nevertheless, this co-conformational preference further offers an explanation as to why we do not observe a total of four signals for the α and β protons of the CBPQT^{4+} ring. It stands to reason that, as a consequence of the lack of the usual alongside donor−acceptor interactions involving the BIPY^{2+} units of the CBPQT^{4+} ring and the macrocyclic polyether that arise from this distinctive co-conformation, the degenerate pirouetting motion is much faster in comparison[36] with previously studied donor−acceptor catenanes. The hypothesis associated with this fast pirouetting motion is also supported by the observation of only three signals, instead of six, arising from the protons associated with the DNP unit at all the temperatures investigated.

In order to investigate the dynamic motion associated with the degenerate rotations of the DNP and BIPY^{2+} units of the CBPQT^{4+} ring, ^{1}H NMR spectroscopy was carried out at a range of temperatures for both cases in CD_3CN over a range of 253 to 333 K. The resonances associated with the α and β protons of the BIPY^{2+} units, along with the methyl (H_{CH_2}) and phenylene (H_{Ar}) groups of the CBPQT^{4+} ring in $\mathbf{6}^{6+}$ were all observed to undergo broadening, coalescence, and sharpening up again as the temperature was increased from 253 to 333 K (Figure 5). The coalescences for the α, β, methylene, and phenylene protons were all observed to occur at different temperatures. These observations are consistent with the degenerate rotation[37] of the DNP and BIPY^{2+} units of the CBPQT^{4+} ring. By calculating[38] the rate of exchange (k_c) at the different coalescence temperatures (T_c) associated with the different sets of exchanging protons, the enthalpic ($\Delta H^{\ddagger}$) and entropic ($\Delta S^{\ddagger}$) contributions to the free energy barrier ($\Delta G^{\ddagger}$) governing the degenerate rotations can be obtained for $\mathbf{6}\cdot 6PF_6$. The free energy barrier $\Delta G^{\ddagger}$ was found to be 14.4 kcal mol^{-1}. The free energy barrier of the transition state for this motion is associated (Figure 6) with an enthalpy of activation equal to 11.1 kcal mol^{-1} and is disfavored entropically by −11.1 cal mol^{-1} K^{-1}. In the case of $\mathbf{7}^{6+}$, the close proximity of the positively charged BIPY^{2+} unit in the crown ether to the CBPQT^{4+} ring increases the free energy barrier to the circumrotational processes, most likely as a result of both increased steric interactions and Coulombic forces. We believe that both of these factors conspire together to raise[39] the free energy barrier ($\Delta G^{\ddagger}$ = 17.0 kcal mol^{-1}), leading to the elevated coalescence temperatures observed (see SI) for $\mathbf{7}\cdot 6PF_6$.

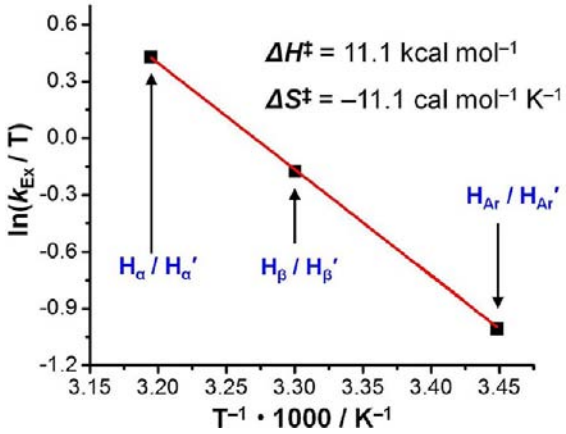

Figure 6. Eyring plot using the rate of exchange (pirouetting, k_{Ex}) obtained from different pairs of protons undergoing site exchanges at different coalescence temperatures. The slope of the best-fit line is proportional to a free enthalpy of activation of $\Delta H^{\ddagger}$, and the intercept affords the free entropy of activation $\Delta S^{\ddagger}$.

Electrochemistry. The redox-activated switching processes for $\mathbf{6}^{6+}$ and $\mathbf{7}^{6+}$ were characterized (Figure 7) by cyclic voltammetry (CV) and square-wave differential pulse voltammetry (DPV). The BIPY^{2+} unit of the macrocyclic polyether serves as a recognition unit, provided both it and the CBPQT^{4+} ring are reduced to their radical cationic forms. The crown ethers $\mathbf{3}^{2+}$ and $\mathbf{5}^{2+}$, containing in each case only one BIPY^{2+} unit, undergo (see SI) two consecutive reversible one-electron processes, $\mathbf{3}^{2+}\rightarrow\mathbf{3}^{(\bullet+)}$ and $\mathbf{5}^{2+}\rightarrow\mathbf{5}^{(\bullet+)}$ (−0.40 and −0.37 V at peak potential) and $\mathbf{3}^{(\bullet+)}\rightarrow\mathbf{3}$ and $\mathbf{5}^{(\bullet+)}\rightarrow\mathbf{5}$ (−0.83 V at peak potential), while the free CBPQT^{4+} ring with its two BIPY^{2+} units exhibits (see SI) two consecutive reversible two-electron processes, CBPQT$^{4+}\rightarrow$CBPQT$^{2(\bullet+)}$ (−0.30 V at peak potential) and CBPQT$^{2(\bullet+)}\rightarrow$CBPQT (−0.73 V at peak potential). The reduction of the [2]catenane $\mathbf{6}^{6+}$ to its trisradical tricationic

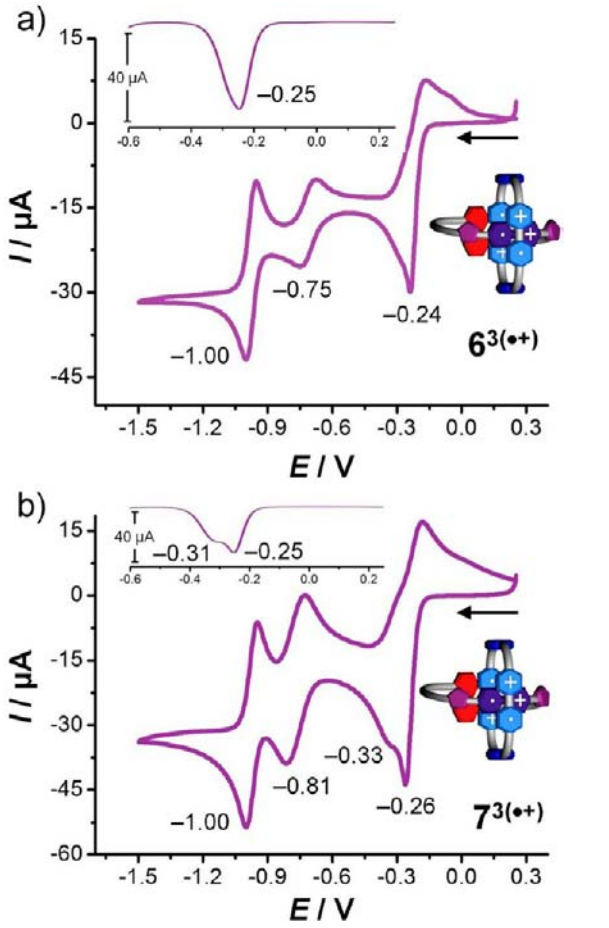

Figure 7. (a) Cyclic voltammogram recorded on a solution of $\mathbf{6}\cdot 6PF_6$ (MeCN, 1 mM, 298 K, 10 mV s^{-1}). The inset shows the square-wave DPV of $\mathbf{6}\cdot 6PF_6$ recorded for the first redox process. (b) Cyclic voltammogram recorded on a solution of $\mathbf{7}\cdot 6PF_6$ (MeCN, 1 mM, 298 K, 50 mV s^{-1}). The inset shows the square-wave DPV of $\mathbf{7}\cdot 6PF_6$ recorded in the region of the first two redox processes.

dx.doi.org/10.1021/ja3037355 | J. Am. Chem. Soc. 2012, 134, 11709−11720

form is observed to proceed (Figure 7a) as a single three-electron redox process. The reduction peak at −0.24 V, which corresponds to this three-electron process, can be assigned to three one-electron reductions—two electrons being transferred to the LUMOs of the two $BIPY^{2+}$ units of the $CBPQT^{4+}$ ring ($CBPQT^{4+}\rightarrow CBPQT^{2(\bullet+)}$), and the other electron to the LUMO of $BIPY^{2+}$ unit of the macrocyclic polyether component. This reduction potential is shifted positively compared to both those of the free macrocycle $\mathbf{3}\cdot 2PF_6$ and $CBPQT\cdot 4PF_6$ as a consequence of the stability of the $BIPY^{\bullet+}$ radical−radical interactions which occur in the trisradical tricationic form of $\mathbf{6}^{6+}$. A consequence of this three-electron reduction is that the diradical dicationic $CBPQT^{2(\bullet+)}$ ring encircles the $BIPY^{\bullet+}$ radical cation of the macrocyclic polyether, stabilized by radical−radical interactions. Evidence for this co-conformational state can be ascertained by analysis of the reduction processes which lead to the fully reduced (neutral) form of the catenane. The second reduction peak (−0.75 V) can be assigned to the one-electron reduction of the $BIPY^{\bullet+}$ unit of the $CBPQT^{2(\bullet+)}$ ring ($CBPQT^{2(\bullet+)}\rightarrow CBPQT^{\bullet+}$) which is not as strongly engaged in radical−radical interactions with the $BIPY^{\bullet+}$ radical cation of the macrocyclic polyether based on the hypothesis that the spin of its radical electron is left unpaired. The third two-electron reduction peak observed at −1.00 V can be attributed to two simultaneous one-electron reductions ($CBPQT^{(\bullet+)}\rightarrow CBPQT$ and $3^{(\bullet+)}/3$) of the two spin-paired $BIPY^{\bullet+}$ units. Because of this favorable radical pairing between the two $BIPY^{\bullet+}$ radical cations, the last reduction process is shifted to a substantially more negative value, compared to the second reduction peaks of the free $CBPQT^{4+}$ and macrocyclic polyether 3^{2+} observed at −0.73 and −0.83 V, respectively. The existence of this negative shift is characteristic of the encirclement of $CBPQT^{2(\bullet+)}$ around the $BIPY^{\bullet+}$ unit of the crown ether component. The return scan shows that all three of these reduction processes are reversible, at least on the time scale of the experiment in question. Reoxidation of the trisradical tricationic form of $\mathbf{6}^{6+}$ reinstates favorable donor−acceptor interactions resulting in a return to the ground-state co-conformation in which the $CBPQT^{4+}$ ring encircles exclusively the DNP unit.

On the other hand, the CV of the smaller [2]catenane $\mathbf{7}\cdot 6PF_6$ reveals (Figure 7b) four consecutive reversible redox processes. Because of the smaller size of the macrocyclic polyether, reduction of $\mathbf{7}^{6+}$ to its trisradical tricationic form occurs over two discrete redox processes, both of which were confirmed by DPV. The first reduction peak observed at −0.26 V, which corresponds to a two-electron process, can be assigned to two one-electron reductions—one electron being transferred to one of the $BIPY^{2+}$ units of the $CBPQT^{4+}$ ring ($CBPQT^{4+}\rightarrow CBPQT^{(2+)(\bullet+)}$), and the other to the $BIPY^{2+}$ unit of the crown ether component ($\mathbf{5}^{2+}\rightarrow\mathbf{5}^{\bullet+}$). We hypothesize that the constrained geometry of the macrocyclic polyether stabilizes—either kinetically or thermodynamically—this bis-radical tetracationic co-conformation, in which the DNP unit resides inside the cavity of the $CBPQT^{(2+)(\bullet+)}$ ring, even if only on a time scale that is long compared to that of the experiment. As a result, the reduction of the dicationic $BIPY^{2+}$ unit of the $CBPQT^{(2+)(\bullet+)}$ ring occurs as a separate redox-process observed at −0.33 V (peak potential), generating the trisradical form of the catenane. We hypothesize the $CBPQT^{2(\bullet+)}$ ring now moves from the DNP unit and encircles the $BIPY^{\bullet+}$ radical cation as a consequence of favorable radical−radical interactions that ensue. The third reduction peak (−0.81 V) can be assigned to the one-electron reduction of the unpaired $BIPY^{\bullet+}$ unit of the $CBPQT^{2(\bullet+)}$ ring ($CBPQT^{2(\bullet+)}\rightarrow CBPQT^{(\bullet+)}$). The fourth reduction peak (−1.00 V) can be attributed to two simultaneous one-electron reductions of the spin-paired $BIPY^{\bullet+}$ radical cations. At a scan rate of 50 mV s^{-1}, all of these redox processes appear to be reversible.

UV/Vis Spectroscopy. The free crown ethers $\mathbf{3}\cdot 2PF_6$ and $\mathbf{5}\cdot 2PF_6$ as well as the [2]catenanes $\mathbf{6}\cdot 6PF_6$ and $\mathbf{7}\cdot 6PF_6$ were all characterized (Figure 8) by UV/vis spectroscopy employing

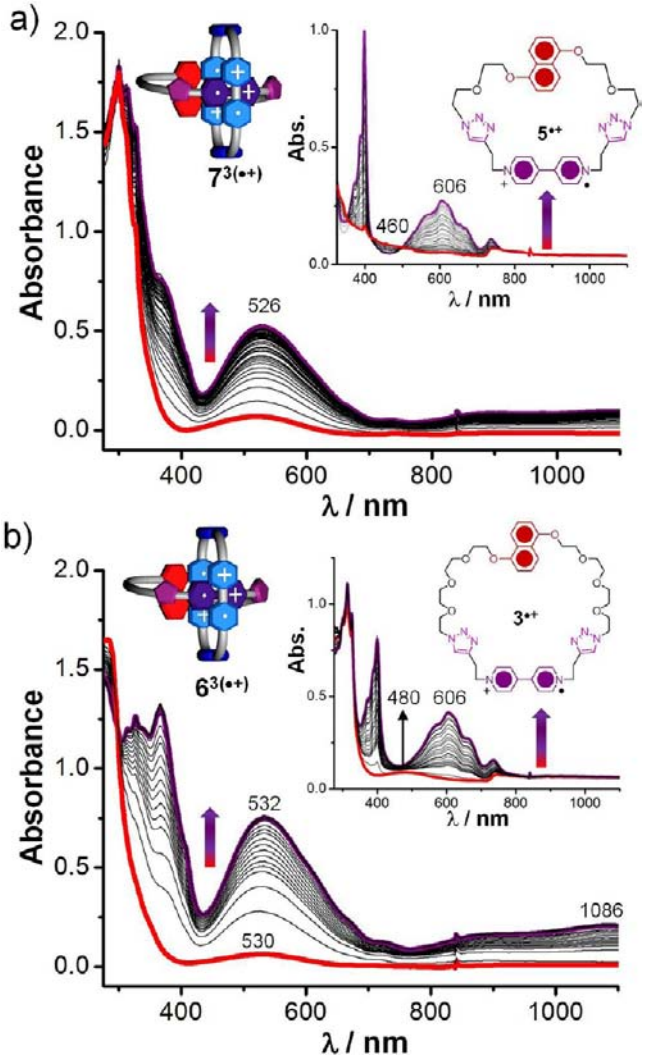

Figure 8. Results of spectroelectrochemistry experiments recorded on a solution of (a) $\mathbf{6}\cdot 6PF_6$ and (b) $\mathbf{7}\cdot 6PF_6$ (MeCN, 0.25 mM, 298 K, −0.5 V potential). The insets show the results from their free macrocyclic components $\mathbf{3}\cdot 2PF_6$ and $\mathbf{5}\cdot 2PF_6$, respectively, recorded under identical conditions.

spectroelectrochemical techniques in MeCN solutions. Intramolecular donor−acceptor interactions between the DNP and $BIPY^{2+}$ units in the crown ethers $\mathbf{3}^{2+}$ and $\mathbf{5}^{2+}$ were confirmed by the broad charge-transfer band centered around 490 nm with molar absorptivities of 2.28×10^4 m^2 mol^{-1} for both macrocyclic polyethers. The maximum intensities of the charge-transfer bands were red-shifted to 534 nm in the case of the [2]catenanes $\mathbf{6}^{6+}$ and $\mathbf{7}^{6+}$ and gave corresponding molar absorptivities of 6.72×10^4 and 1.02×10^5 m^2 mol^{-1}, respectively.

dx.doi.org/10.1021/ja3037355 | J. Am. Chem. Soc. 2012, 134, 11709−11720

Application of a −0.5 V potential to solutions of the two crown ethers $\mathbf{3}^{2+}$ and $\mathbf{5}^{2+}$, as well as of the [2]catenanes $\mathbf{6}^{6+}$ and $\mathbf{7}^{6+}$, resulted in significant changes to the UV/vis region of the absorption spectra consistent with the formation of $BIPY^{\bullet+}$ radical cations. The resulting dark purple solutions of $\mathbf{6}^{6+}$ and $\mathbf{7}^{6+}$, however, display absorption bands centered around ∼530 nm as well as broad bands of lesser intensities in the NIR, both of which are consistent with the absorption spectra of the $BIPY^{\bullet+}$ radical cations in their "pimerized" [40] forms, previously observed[18,33,34] in both supramolecular and mechanically interlocked systems employing $BIPY^{\bullet+}$ radical−radical interactions. These characteristic maximum absorptions support the conclusions drawn from the CV and X-ray crystallographic data that encirclement of the $CBPQT^{2(\bullet+)}$ ring around the $BIPY^{\bullet+}$ radical cation unit of the macrocyclic polyether occurs after a three-electron reduction for both $\mathbf{6}^{6+}$ and $\mathbf{7}^{6+}$. By contrast, the absorption spectra for the free $CBPQT^{4+}$ ring as well as the free crown ethers $\mathbf{3}^{2+}$ and $\mathbf{5}^{2+}$ exhibit an intense absorption band (λ_{max} = 603 nm) characteristic of $BIPY^{\bullet+}$ radical cations existing in their monomeric forms.

EPR Spectroscopy. The trisradical tricationic redox state of the two [2]catenanes − $\mathbf{6}^{3(\bullet+)}$ and $\mathbf{7}^{3(\bullet+)}$ − as well as the radical cationic states of their free components, were investigated (Figure 9) further by EPR spectroscopy in MeCN at 298 K. Both macrocycles $\mathbf{3}^{\bullet+}$ and $\mathbf{5}^{\bullet+}$ display well-resolved hyperfine splitting in their EPR spectra, indicating that both of these compounds exist in low spin-exchange regimes. The macrocycle $\mathbf{5}^{\bullet+}$ shows a broader spectrum than does $\mathbf{3}^{\bullet+}$, an observation which can be explained by the slower tumbling rate in the case of the larger macrocycle, namely $\mathbf{3}^{\bullet+}$. The free $CBPQT^{2(\bullet+)}$ ring is also in a high spin exchange regime as a result of intramolecular interactions between its two constituent $BIPY^{\bullet+}$ units. The trisradical tricationic [2]catenanes $\mathbf{6}^{3(\bullet+)}$ and $\mathbf{7}^{3(\bullet+)}$ afford spectra that are fully broadened, with no discernible hyperfine splitting, indicating an intramolecular spin exchange interaction between the $CBPQT^{2(\bullet+)}$ diradical dication and the $BIPY^{\bullet+}$ units of the macrocyclic polyethers. The observations of a lack of hyperfine splitting are completely consistent[18a] with the previously reported bistable [2]rotaxanes made to switch by employing radical−radical interactions.

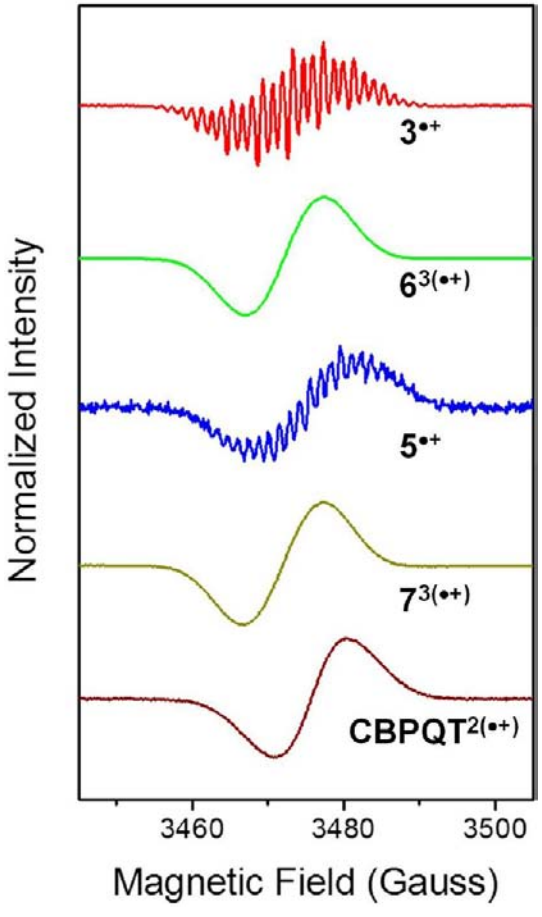

Figure 9. EPR spectra obtained from solutions (MeCN, 1 mM, 298 K) of the trisradical tricationic forms of $\mathbf{6}\cdot 6PF_6$ and $\mathbf{7}\cdot 6PF_6$ as well as the radical cationic forms of their free components recorded under identical conditions.

CONCLUSIONS

In a nutshell, we have introduced a design strategy for obtaining bistable [2]catenanes that exist not as a distribution of co-conformations in either their ground or switched states, but rather as single co-conformations. By employing donor−acceptor interactions together with Coulombic repulsions in the ground state, a single co-conformation can be attained. By taking advantage of radical−radical interactions to obtain the switched state, and thereby nullifying the donor−acceptor recognition, leading once again to only one co-conformation. We have provided evidence in solution in the form of ^{1}H NMR, UV/vis, and EPR spectroscopic data as well as experiments of an electrochemical nature in order to demonstrate the operation of this all-or-nothing switching. The lack of a distribution of co-conformations is in stark contrast to the mechanism of switching of the more typical redox-active bistable MIMs in the literature which have relied almost exclusively on two different donor units, one with a greater affinity for the electron-deficient ring than the other. Even though a secondary donor unit incorporated into the bistable MIM is usually an order of magnitude or more weaker—by the very nature of the mechanism of switching implicit in the design—some of the co-conformation involving encirclement of the weaker donor must exist to some extent. Establishing a mechanism of switching, which leads to a single and exclusive population of just one co-conformation in both the ground and switched states, has positive implications for applications which utilize the mechanical motions of these bistable MIMs to achieve some desired function. When considering applications in the context of solid-state molecular electronic devices, the radical states of these bistable [2]catenanes in their single crystalline forms may possess more complex and unique transport properties than those typically observed for the more thoroughly investigated closed-shell organic semiconductors. Future work is necessary in devising synthetic protocols that will increase the yields of these [2]catenanes. High-yielding synthetic procedures, which could rely[33] on radical templation, are a requirement if these mechanically interlocked molecules are to be integrated into molecular and bulk electronic devices.

ASSOCIATED CONTENT

Supporting Information

Full details of instrumentation and analytical techniques; synthesis and characterization data for self-complexing macrocycles $\mathbf{3}\cdot 2PF_6$ and $\mathbf{5}\cdot 2PF_6$ and for [2]catenanes $\mathbf{6}\cdot 6PF_6$ and $\mathbf{7}\cdot 6PF_6$; crystallographic data for macrocycles $\mathbf{3}\cdot Ni(mnt)_2$ and $\mathbf{5}\cdot 2PF_6$, for [2]catenanes $\mathbf{6}\cdot 6PF_6$ and $\mathbf{7}\cdot 6PF_6$, and for the trisradical state of $\mathbf{7}^{3(\bullet+)}\cdot 3PF_6$; ^{1}H NMR complexation study of

dx.doi.org/10.1021/ja3037355 | J. Am. Chem. Soc. 2012, 134, 11709−11720

1·2PF_6, **2**, and **CBPQT**·4PF_6; solid-state structures of **3**·2PF_6 and **5**·2PF_6; ^{1}H−^{1}H COSY and variable-temperature ^{1}H NMR spectroscopic investigation of the [2]catenanes **6**·6PF_6 and **7**·6PF_6; cyclic voltammograms of **3**·2PF_6, **5**·2PF_6, and **CBPQT**·4PF_6. This material is available free of charge via the Internet at http://pubs.acs.org.

AUTHOR INFORMATION

Corresponding Author

stoddart@northwestern.edu

Notes

The authors declare no competing financial interest.

ACKNOWLEDGMENTS

The research reported in this paper is based upon work supported under the auspices of an international collaboration supported in the U.S. by the National Science Foundation under Grant No. CHE-0924620 and in the U.K. by the Engineering and Physical Sciences Research Council under Grant No. EP/H003517/1. A.C.F., J.C.B., and J.F.S. were supported by the WCU Program (NRFR-31-2008-000-10055-0) funded by the Ministry of Education, Science and Technology, Korea. A.C.F. acknowledges support from an NSF Graduate Research Fellowship. M.R.W. acknowledges support by the National Science Foundation under Grant CHE-1012378. R.C. was supported as part of the ANSER Center, an Energy Frontier Research Center funded by the U.S. Department of Energy, Office of Science, Office of Basic Energy Sciences, under award no. DE-SC0001059.

REFERENCES

(1) (a) Deutman, A. B.; Monnereau, C.; Moalin, M.; Coumans, R. G. E.; Veling, N.; Coenen, M.; Smits, J. M. M.; de, G. R.; Elemans, J. A. A. W.; Ercolani, G.; Nolte, R. J. M.; Rowan, A. E. *Proc. Natl. Acad. Sci. U.S.A.* **2009**, *106*, 10471. (b) Ellermann, M.; Jakob-Roetne, R.; Lerner, C.; Borroni, E.; Schlatter, D.; Roth, D.; Ehler, A.; Rudolph, M. G.; Diederich, F. *Angew. Chem., Int. Ed.* **2009**, *48*, 9092. (c) Inokuma, Y.; Arai, T.; Fujita, M. *Nat. Chem.* **2010**, *2*, 780. (d) Joyce, L. A.; Shabbir, S. H.; Anslyn, E. V. *Chem. Soc. Rev.* **2010**, *39*, 3621.

(2) (a) Whitesides, G. M.; Mathias, J. P.; Seto, C. T. *Science* **1991**, *254*, 1312. (b) Philp, D.; Stoddart, J. F. *Angew. Chem., Int. Ed. Engl.* **1996**, *35*, 1155. (c) Williams, A. R.; Northrop, B. H.; Chang, T.; Stoddart, J. F.; White, A. J. P.; Williams, D. J. *Angew. Chem., Int. Ed.* **2006**, *45*, 6665. (d) Desigaux, L.; Sainlos, M.; Lambert, O.; Chevre, R.; Letrou-Bonneval, E.; Vigneron, J.-P.; Lehn, P.; Lehn, J.-M.; Pitard, B. *Proc. Natl. Acad. Sci. U.S.A.* **2007**, *104*, 16534. (e) Lledo, A.; Kamioka, S.; Sather, A. C.; Rebek, J., Jr. *Angew. Chem., Int. Ed.* **2011**, *50*, 1299. (f) Chakrabarty, R.; Mukherjee, P. S.; Stang, P. J. *Chem. Rev.* **2011**, *111*, 6810.

(3) (a) Kim, K. *Chem. Soc. Rev.* **2002**, *31*, 96. (b) Rijs, A. M.; Compagnon, I.; Oomens, J.; Hannam, J. S.; Leigh, D. A.; Buma, W. J. *J. Am. Chem. Soc.* **2009**, *131*, 2428. (c) Crowley, J. D.; Goldup, S. M.; Lee, A.-L.; Leigh, D. A.; McBurney, R. T. *Chem. Soc. Rev.* **2009**, *38*, 1530. (d) Li, S.; Liu, M.; Zheng, B.; Zhu, K.; Wang, F.; Li, N.; Zhao, X.-L.; Huang, F. *Org. Lett.* **2009**, *11*, 3350. (e) Mateo-Alonso, A. *Chem. Commun.* **2010**, 9089. (f) Qu, D.-H.; Tian, H. *Chem. Sci.* **2011**, *2*, 1011. (g) Beves, J. E.; Blight, B. A.; Campbell, C. J.; Leigh, D. A.; McBurney, R. T. *Angew. Chem., Int. Ed.* **2011**, *50*, 9260.

(4) (a) Gunter, M. J.; Hockless, D. C. R.; Johnston, M. R.; Skelton, B. W.; White, A. H. *J. Am. Chem. Soc.* **1994**, *116*, 4810. (b) Zhu, X.-Z.; Chen, C.-F. *J. Am. Chem. Soc.* **2005**, *127*, 13158. (c) Wang, W.; Wang, L.; Palmer, B. J.; Exarhos, G. J.; Li, A. D. Q. *J. Am. Chem. Soc.* **2006**, *128*, 11150. (d) Cheng, P.-N.; Huang, P.-Y.; Li, W.-S.; Ueng, S.-H.; Hung, W.-C.; Liu, Y.-H.; Lai, C.-C.; Wang, Y.; Peng, S.-M.; Chao, I.; Chiu, S.-H. *J. Org. Chem.* **2006**, *71*, 2373. (e) Roithova, J.; Milko, P.; Ricketts, C. L.; Schroeder, D.; Besson, T.; Dekoj, V.; Bělohradsky, M. *J. Am. Chem. Soc.* **2007**, *129*, 10141. (f) Halterman, R. L.; Pan, X.; Martyn, D. E.; Moore, J. L.; Long, A. T. *J. Org. Chem.* **2007**, *72*, 6454. (g) Megiatto, J. D., Jr.; Schuster, D. I. *J. Am. Chem. Soc.* **2008**, *130*, 12872. (h) Niu, Z.; Gibson, H. W. *Chem. Rev.* **2009**, *109*, 6024. (i) Megiatto, J. D., Jr.; Schuster, D. I. *Chem.—Eur. J.* **2009**, *15*, 5444. (j) Beyler, M.; Heitz, V.; Sauvage, J.-P. *J. Am. Chem. Soc.* **2010**, *132*, 4409. (k) Evans, N. H.; Serpell, C. J.; Beer, P. D. *Angew. Chem., Int. Ed.* **2011**, *50*, 2507. (l) Yang, W.; Li, Y.; Zhang, J.; Chen, N.; Chen, S.; Liu, H.; Li, Y. *J. Org. Chem.* **2011**, *76*, 7750. (m) Cougnon, F. B. L.; Au-Yeung, H. Y.; Pantos, G. D.; Sanders, J. K. M. *J. Am. Chem. Soc.* **2011**, *133*, 3198.

(5) (a) Anderson, S.; Anderson, H. L. *Angew. Chem., Int. Ed. Engl.* **1996**, *35*, 1956. (b) Vignon, S. A.; Jarrosson, T.; Iijima, T.; Tseng, H.-R.; Sanders, J. K. M.; Stoddart, J. F. *J. Am. Chem. Soc.* **2004**, *126*, 9884. (c) Arunkumar, E.; Forbes, C. C.; Noll, B. C.; Smith, B. D. *J. Am. Chem. Soc.* **2005**, *127*, 3288. (d) Rescifina, A.; Zagni, C.; Iannazzo, D.; Merino, P. *Curr. Org. Chem.* **2009**, *13*, 448. (e) Haenni, K. D.; Leigh, D. A. *Chem. Soc. Rev.* **2010**, *39*, 1240. (f) Olsen, J.-C.; Fahrenbach, A. C.; Trabolsi, A.; Friedman, D. C.; Dey, S. K.; Gothard, C. M.; Shveyd, A. K.; Gasa, T. B.; Spruell, J. M.; Olson, M. A.; Wang, C.; Jacquot de Rouville, H.-P.; Botros, Y. Y.; Stoddart, J. F. *Org. Biomol. Chem.* **2011**, *9*, 7126. (g) Dey, S. K.; Coskun, A.; Fahrenbach, A. C.; Barin, G.; Basuray, A. N.; Trabolsi, A.; Botros, Y. Y.; Stoddart, J. F. *Chem. Sci.* **2011**, *2*, 1046. (h) Yang, W.; Li, Y.; Liu, H.; Chi, L.; Li, Y. *Small* **2012**, *8*, 504.

(6) (a) Chichak, K. S.; Cantrill, S. J.; Pease, A. R.; Chiu, S.-H.; Cave, G. W. V.; Atwood, J. L.; Stoddart, J. F. *Science* **2004**, *304*, 1308. (b) Meyer, C. D.; Forgan, R. S.; Chichak, K. S.; Peters, A. J.; Tangchaivang, N.; Cave, G. W. V.; Khan, S. I.; Cantrill, S. J.; Stoddart, J. F. *Chem.—Eur. J.* **2010**, *16*, 12570.

(7) (a) Lukin, O.; Vögtle, F. *Angew. Chem., Int. Ed.* **2005**, *44*, 1456. (b) Pentecost, C. D.; Chichak, K. S.; Peters, A. J.; Cave, G. W. V.; Cantrill, S. J.; Stoddart, J. F. *Angew. Chem., Int. Ed.* **2007**, *46*, 218. (c) Peinador, C.; Blanco, V.; Quintela, J. M. *J. Am. Chem. Soc.* **2009**, *131*, 920.

(8) (a) Aricó, F.; Badjic, J. D.; Cantrill, S. J.; Flood, A. H.; Leung, K. C. F.; Liu, Y.; Stoddart, J. F. *Top. Curr. Chem.* **2005**, *249*, 203. (b) Griffiths, K. E.; Stoddart, J. F. *Pure Appl. Chem.* **2008**, *80*, 485. (c) Stoddart, J. F.; Colquhoun, H. M. *Tetrahedron* **2008**, *64*, 8231. (d) Stoddart, J. F. *Chem. Soc. Rev.* **2009**, *38*, 1802.

(9) (a) Chang, S. K.; Hamilton, A. D. *J. Am. Chem. Soc.* **1988**, *110*, 1318. (b) Reinhoudt, D. N.; Crego-Calama, M. *Science* **2002**, *295*, 2403. (c) Au-Yeung, H. Y.; Pantos, G. D.; Sanders, J. K. M. *Proc. Natl. Acad. Sci. U.S.A.* **2009**, *106*, 10466. (d) Bastings, M. M. C.; de Greef, T. F. A.; van Dongen, J. L. J.; Merkx, M.; Meijer, E. W. *Chem. Sci.* **2010**, *1*, 79. (e) Gong, H.-Y.; Rambo, B. M.; Cho, W.; Lynch, V. M.; Oh, M.; Sessler, J. L. *Chem. Commun.* **2011**, 5973.

(10) Fyfe, M. C. T.; Stoddart, J. F. *Acc. Chem. Res.* **1997**, *30*, 393.

(11) (a) Odell, B.; Reddington, M. V.; Slawin, A. M. Z.; Spencer, N.; Stoddart, J. F.; Williams, D. J. *Angew. Chem., Int. Ed. Engl.* **1988**, *27*, 1547. (b) Brown, C. L.; Philp, D.; Stoddart, J. F. *Synlett* **1991**, 462. (c) Asakawa, M.; Dehaen, W.; L'abbé, G.; Menzer, S.; Nouwen, J.; Raymo, F. M.; Stoddart, J. F.; Williams, D. J. *J. Org. Chem.* **1996**, *61*, 9591. (d) Sue, C.-H.; Basu, S.; Fahrenbach, A. C.; Shveyd, A. K.; Dey, S. K.; Botros, Y. Y.; Stoddart, J. F. *Chem. Sci.* **2010**, *1*, 119.

(12) (a) Green, J. E.; Choi, J. W.; Boukai, A.; Bunimovich, Y.; Johnston-Halperin, E.; DeIonno, E.; Luo, Y.; Sheriff, B. A.; Xu, K.; Shin, Y. S.; Tseng, H.-R.; Stoddart, J. F.; Heath, J. R. *Nature* **2007**, *445*, 414. (b) Coskun, A.; Banaszak, M.; Astumian, R. D.; Stoddart, J. F.; Grzybowski, B. A. *Chem. Soc. Rev.* **2012**, *41*, 191.

(13) (a) Juluri, B. K.; Kumar, A. S.; Liu, Y.; Ye, T.; Yang, Y.-W.; Flood, A. H.; Fang, L.; Stoddart, J. F.; Weiss, P. S.; Huang, T. J. *ACS Nano* **2009**, *3*, 291. (b) Coskun, A.; Spruell, J. M.; Barin, G.; Dichtel, W. R.; Flood, A. H.; Botros, Y. Y.; Stoddart, J. F. *Chem. Soc. Rev.* **2012**, *41*, 4827.

(14) Klajn, R.; Fang, L.; Coskun, A.; Olson, M. A.; Wesson, P. J.; Stoddart, J. F.; Grzybowski, B. A. *J. Am. Chem. Soc.* **2009**, *131*, 4233.

(15) (a) Ashton, P. R.; Bissell, R. A.; Spencer, N.; Stoddart, J. F.; Tolley, M. S. *Synlett* **1992**, 923. (b) Bissell, R. A.; Córdova, E.; Kaifer, A. E.; Stoddart, J. F. *Nature* **1994**, *369*, 133. (c) Asakawa, M.; Ashton, P. R.; Balzani, V.; Credi, A.; Hamers, C.; Mattersteig, G.; Montalti, M.; Shipway, A. N.; Spencer, N.; Stoddart, J. F.; Tolley, M. S.; Venturi, M.; White, A. J. P.; Williams, D. J. *Angew. Chem., Int. Ed.* **1998**, *37*, 333. (d) Collier, C. P.; Mattersteig, G.; Wong, E. W.; Luo, Y.; Beverly, K.; Sampaio, J.; Raymo, F. M.; Stoddart, J. F.; Heath, J. R. *Science* **2000**, *289*, 1172. (e) Spruell, J. M.; Paxton, W. F.; Olsen, J.-C.; Benítez, D.; Tkatchouk, E.; Stern, C. L.; Trabolsi, A.; Friedman, D. C.; Goddard, W. A., III; Stoddart, J. F. *J. Am. Chem. Soc.* **2009**, *131*, 11571.

(16) (a) Choi, J. W.; Flood, A. H.; Steuerman, D. W.; Nygaard, S.; Braunschweig, A. B.; Moonen, N. N. P.; Laursen, B. W.; Luo, Y.; DeIonno, E.; Peters, A. J.; Jeppesen, J. O.; Xu, K.; Stoddart, J. F.; Heath, J. R. *Chem.—Eur. J.* **2005**, *12*, 261. (b) Fahrenbach, A. C.; Barnes, J. C.; Li, H.; Benitez, D.; Basuray, A. N.; Fang, L.; Sue, C.-H.; Barin, G.; Dey, S. K.; Goddard, W. A., III; Stoddart, J. F. *Proc. Natl. Acad. Sci. U.S.A.* **2011**, *108*, 20416.

(17) Cao, D.; Amelia, M.; Klivansky, L. M.; Koshkakaryan, G.; Khan, S. I.; Semeraro, M.; Silvi, S.; Venturi, M.; Credi, A.; Liu, Y. *J. Am. Chem. Soc.* **2010**, *132*, 1110.

(18) (a) Trabolsi, A.; Khashab, N.; Fahrenbach, A. C.; Friedman, D. C.; Colvin, M. T.; Coti, K. K.; Benítez, D.; Tkatchouk, E.; Olsen, J.-C.; Belowich, M. E.; Carmielli, R.; Khatib, H. A.; Goddard, W. A., III; Wasielewski, M. R.; Stoddart, J. F. *Nat. Chem.* **2010**, *2*, 42. (b) Fahrenbach, A. C.; Barnes, J. C.; Lanfranchi, D. A.; Li, H.; Coskun, A.; Gassensmith, J. J.; Liu, Z.; Benítez, D.; Trabolsi, A.; Goddard, W. A.; Elhabiri, M.; Stoddart, J. F. *J. Am. Chem. Soc.* **2012**, *134*, 3061.

(19) (a) Chia, S.; Cao, J.; Stoddart, J. F.; Zink, J. I. *Angew. Chem., Int. Ed.* **2001**, *40*, 2447. (b) Hernandez, R.; Tseng, H.-R.; Wong, J. W.; Stoddart, J. F.; Zink, J. I. *J. Am. Chem. Soc.* **2004**, *126*, 3370. (c) Saha, S.; Johansson, L. E.; Flood, A. H.; Tseng, H.-R.; Zink, J. I.; Stoddart, J. F. *Small* **2005**, *1*, 87. (d) Saha, S.; Johansson, E.; Flood, A. H.; Tseng, H.-R.; Zink, J. I.; Stoddart, J. F. *Chem.—Eur. J.* **2005**, *11*, 6846. (e) Nguyen, T. D.; Leung, K. C-F.; Liong, M.; Liu, Y.; Stoddart, J. F.; Zink, J. I. *Adv. Funct. Mater.* **2007**, *17*, 2101.

(20) (a) Ghosh, P.; Federwisch, G.; Kogej, M.; Schalley, C. A.; Haase, D.; Saak, W.; Ltzen, A.; Gschwind, R. M. *Org. Biomol. Chem.* **2005**, *3*, 2691. (b) Brough, B.; Northrop, B. H.; Schmidt, J. J.; Tseng, H.-R.; Houk, K. N.; Stoddart, J. F.; Ho, C.-M. *Proc. Natl. Acad. Sci. U.S.A.* **2006**, *103*, 8583. (c) Trabolsi, A.; Fahrenbach, A. C.; Dey, S. K.; Share, A. I.; Friedman, D. C.; Basu, S.; Gasa, T. B.; Khashab, N. M.; Saha, S.; Aprahamian, I.; Khatib, H. A.; Flood, A. H.; Stoddart, J. F. *Chem. Commun.* **2010**, *46*, 871. (d) Li, H.; Zhao, Y.-L.; Fahrenbach, A. C.; Kim, S.-Y.; Paxton, W. F.; Stoddart, J. F. *Org. Biomol. Chem.* **2011**, *9*, 2240. (e) Hmadeh, M.; Fahrenbach, A. C.; Basu, S.; Trabolsi, A.; Benítez, D.; Li, H.; Albrecht-Gary, A.-M.; Elhabiri, M.; Stoddart, J. F. *Chem.—Eur. J.* **2011**, *17*, 6076.

(21) (a) Huisgen, R. *Pure Appl. Chem.* **1989**, *61*, 613. (b) Rostovtsev, V. V.; Green, L. G.; Fokin, V. V.; Sharpless, K. B. *Angew. Chem., Int. Ed.* **2002**, *41*, 2596. (c) Tornøe, C. W.; Christensen, C.; Meldal, M. *J. Org. Chem.* **2002**, *67*, 3057. (d) Fahrenbach, A. C.; Stoddart, J. F. *Chem. Asian. J.* **2011**, *6*, 2660.

(22) Although a recent report (Tejerina, B.; Gothard, C. M.; Grzybowski, B. A. *Chem.—Eur. J.* **2012**, *18*, 5606.) on the subject of theoretical calculations suggests that charge transfer occurs only in the case of side-on donor−acceptor interactions with one of the $BIPY^{2+}$ units of the $CBPQT^{4+}$ rings and a π-electron-rich donor, overwhelming experimental evidence exists to suggest that charge transfer also occurs in the case of inclusion complexes. See ref 15e and the following: (a) Philp, D.; Slawin, A. M. Z.; Spencer, N.; Stoddart, J. F.; Williams, D. J. *J. Chem. Soc., Chem. Commun.* **1991**, *22*, 1584. (b) Hansen, S. W.; Stein, P. C.; Sørensen, A.; Share, A. I.; Witlicki, E. H.; Kongsted, J.; Flood, A. H.; Jeppesen, J. O. *J. Am. Chem. Soc.* **2012**, *134*, 3857.

(23) (a) Ashton, P. R.; Grognuz, M.; Slawin, A. M. Z.; Stoddart, J. F.; Williams, D. J. *Tetrahedron Lett.* **1991**, *32*, 6235. (b) Belohradsky, M.; Raymo, F. M.; Stoddart, J. F. *Collect. Czech. Chem. Commun.* **1997**, *62*, 527.

(24) Ashton, P. R.; Goodnow, T. T.; Kaifer, A. E.; Reddington, M. V.; Slawin, A. M. Z.; Spencer, N.; Stoddart, J. F.; Vicent, C.; Williams, D. J. *Angew. Chem., Int. Ed. Engl.* **1989**, *28*, 1396.

(25) Crystal data for **6**·6PF_6: $C_{186}H_{215}F_{72}N_{37}O_{16}P_{12}$, M_r = 4964.59, monoclinic, PC_2/c, a = 18.8272(4), b = 20.3121(4), and c = 56.4665(10) Å, β = 95.2940(10)°. V = 21501.8(7) Å^3, T = 100(2) K, Z = 4, D_c = 1.534 g cm^{-3}, μ(Cu Kα) = 2.056 mm^{-1}, F(000) = 10 184; independent measured reflections, 36 766; R_1 = 0.133, wR_2 = 0.425 for 15 547 independent observed reflections [$2\theta \leq 129°$, $I > 2\sigma(I)$]. CCDC 865318.

(26) Crystal data for **7**·6PF_6: $C_{72}H_{80}F_{36}N_{12}O_4P_6 \cdot 3(C_3H_6O)$, M_r = 2155.39, monoclinic, $P2_1/n$, a = 32.7648(17), b = 11.0431(6), and c = 33.1123(16) Å, β = 117.905(3)°. V = 10587.8(9) Å^3, T = 100(2) K, Z = 4, D_c = 1.352 g cm^{-3}, μ(Cu Kα) = 1.971 mm^{-1}, F(000) = 4392; independent measured reflections, 38 858; R_1 = 0.105, wR_2 = 0.294 for 9101 independent observed reflections [$2\theta \leq 124°$, $I > 2\sigma(I)$]. CCDC 865320.

(27) (a) Ashton, P. R.; Brown, C. L.; Chrystal, E. J. T.; Goodnow, T. T.; Kaifer, A. E.; Parry, K. P.; Philp, D.; Slawin, A. M. Z.; Spencer, N.; Stoddart, J. F.; Williams, D. J. *J. Chem. Soc., Chem. Commun.* **1991**, *9*, 634. (b) Wang, C.; Olson, M. A.; Fang, L.; Benítez, D.; Tkatchouk, E.; Basu, S.; Basuray, A. N.; Zhang, D.; Zhu, D.; Goddard, W. A., III; Stoddart, J. F. *Proc. Natl. Acad. Sci. U.S.A.* **2010**, *107*, 13991. (c) Basu, S.; Coskun, A.; Friedman, D. C.; Olson, M. A.; Benítez, D.; Tkachouk, E.; Barin, G.; Young, J.; Fahrenbach, A. C.; Goddard, W. A., III; Stoddart, J. F. *Chem.—Eur. J.* **2011**, *17*, 2107.

(28) Houk, K. N.; Menzer, S.; Newton, S. P.; Raymo, F. M.; Stoddart, J. F.; Williams, D. J. *J. Am. Chem. Soc.* **1999**, *121*, 1479.

(29) Witlicki, E. H.; Hansen, S.; Christensen, M.; Hansen, T.; Nygaard, S.; Jeppesen, J. O.; Wong, E. W.; Jensen, L.; Flood, A. H. *J. Phys. Chem. A* **2009**, *113*, 9450.

(30) Fang, L.; Basu, S.; Sue, C.-H.; Fahrenbach, A. C.; Stoddart, J. F. *J. Am. Chem. Soc.* **2011**, *133*, 396.

(31) Takeshi, E.; Ageishi, K.; Okawara, M. *J. Org. Chem.* **1986**, *51*, 4309.

(32) Crystal data for $7^{3(\bullet+)} \cdot 3PF_6$: $C_{72}H_{72}F_{18}N_{12}O_4P_3$, M = 1604.33, triclinic, $P\bar{1}$, a = 14.0583(3), b = 14.1964(4), and c = 22.7651(6) Å, α = 77.4660(10)°, β = 78.1360(10)°, γ = 86.7390(10)°, V = 4340.02(19) Å^3, T = 100.0(2) K, Z = 2, D_c = 1.228 g cm^{-3}, μ(Cu Kα) = 1.402, F (000) = 1654; independent measured reflections, 31 603; R_1 = 0.086, wR_2 = 0.257 for 12 027 independent observed reflections [$2\theta \leq 134.5°$, $I > 2\sigma(I)$]. CCDC 865321.

(33) Li, H.; Fahrenbach, A. C.; Dey, S. K.; Basu, S.; Trabolsi, A.; Zhu, Z.; Botros, Y. Y.; Stoddart, J. F. *Angew. Chem., Int. Ed.* **2010**, *49*, 8260.

(34) Li, H.; Fahrenbach, A. C.; Coskun, A.; Zhu, Z.; Barin, G.; Zhao, Y.-L.; Botros, Y. Y.; Sauvage, J.-P.; Stoddart, J. F. *Angew. Chem., Int. Ed.* **2011**, *50*, 6782.

(35) It is more difficult to conclude from the experimental data that this same type of co-conformation is being adopted in solution by the larger catenane as well, but it is more likely than a co-conformation which locates the $BIPY^{2+}$ unit of the macrocyclic polyether alongside the $BIPY^{2+}$ unit of the $CBPQT^{4+}$ ring.

(36) For comparison, pirouetting of the $CBPQT^{4+}$ ring around the DNP38C10 ring is slowed down likely as a consequence of the attractive interactions induced by contact between the two electronically complementary DNP and $BIPY^{2+}$ units. See: Asakawa, M.; Ashton, P. R.; Boyd, S. E.; Brown, C. L.; Gillard, R. E.; Kocian, O.; Raymo, F. M.; Stoddart, J. F.; Tolley, M. S.; White, A. J. P.; Williams, D. J. *J. Org. Chem.* **1997**, *62*, 26.

(37) It is important to note that, once the DNP unit leaves the cavity, it is now able to rotate about its O−O axis before re-entering of the $CBPQT^{4+}$ ring. Since no separation of signals is observed in the 4/8, 3/7, and 2/6 protons of the DNP unit, this rotation of the DNP unit associated with free rotation of the $BIPY^{2+}$ units of the $CBPQT^{4+}$ ring is also likely fast on the ^{1}H NMR time scale.

(38) The rate constants, k, at the coalescence temperatures, T_c, were determined using the approximate expression, $k_c = \pi\Delta\nu/2^{1/2}$, where

$\Delta\nu$ is the limiting chemical shift (in Hz) between the exchanging proton resonances. The Eyring equation, $\Delta G_c^{\ddagger} = -RT\ln(k_c h/k_B T_c)$, was used to calculate $\Delta G_c^{\ddagger}$ values at T_c; see: Sutherland, I. O. *Annu. Rep. Nucl. Magn. Reson. Spectrosc.* **1971**, *4*, 71.

(39) This barrier is comparable to that of the smallest reference [2] catenane consisting of DNP-dialkyne macrocyclic polyether mechanically interlocked with the $CBPQT^{4+}$ ring, in which the resonances of the α protons coalesced at 362 K ($\Delta G_c^{\ddagger}$ = 17.5 kcal mol^{-1}). See: Miljanić, O. Š.; Dichtel, W. R.; Khan, S. I.; Mortezaei, S.; Heath, J. R.; Stoddart, J. F. *J. Am. Chem. Soc.* **2007**, *129*, 8236.

(40) (a) Kosower, E. M.; Hajdu, J. *J. Am. Chem. Soc.* **1971**, *93*, 2534. (b) Geuder, W.; Hünig, S.; Suchy, A. *Tetrahedron* **1986**, *42*, 1665.